https://doi.org/10.5194/hess-2020-383
Preprint. Discussion started: 28 July 2020

Hydrology and Earth System Sciences
Discussions
Open Access
EGU

A standardized index for assessing sub-monthly compound dry and hot conditions

Jun Li[1], Zhaoli Wang[1,2], Xushu Wu[1,2,*], Jakob Zscheischler[3,4], Shenglian Guo[5], Xiaohong Chen[6]

[1] *School of Civil Engineering and Transportation, State Key Laboratory of Subtropical Building Science, South China University of Technology, Guangzhou 510641, China.*

[2] *Guangdong Engineering Technology Research Center of Safety and Greenization for Water Conservancy Project, Guangzhou 510641, China.*

[3] *Climate and Environmental Physics, University of Bern, Sidlerstrasse 5, 3012 Bern, Switzerland.*

[4] *Oeschger Centre for Climate Change Research, University of Bern, Bern, Switzerland.*

[5] *State Key Laboratory of Water Resources and Hydropower Engineering Science, Wuhan University, Wuhan 430072, China.*

[6] *Center for Water Resource and Environment, Sun Yat-Sen University, Guangzhou 510275, China*

∗*Correspondence: xshwu@scut.edu.cn.*

https://doi.org/10.5194/hess-2020-383
Preprint. Discussion started: 28 July 2020

Hydrology and Earth System Sciences
Discussions
Open Access
EGU

Abstract: Compound dry and hot conditions pose large impacts on ecosystems and society worldwide. A suite of indices are proposed for the assessments of droughts and heatwaves previously, yet there is no index available for incorporating the joint variability of dry and hot conditions at sub-monthly scale. Here, we introduce a daily-scale index, termed as the standardized compound drought and heat index (SCDHI), to measure the intensity of compound dry and hot conditions. SCDHI is based on the daily drought index (the standardized antecedent precipitation evapotranspiration index (SAPEI)) and the Standardized Temperature Index (STI) and a joint probability distribution method. The new index is verified against real-world compound dry and hot events and the related observed vegetation impacts in China. SCDHI can not only monitor the long-term compound dry and hot events, but also capture such events at sub-monthly scale and reflect the related vegetation activity impacts. The identified compound events generally persisted for 25-35 days and the southern China suffered from compound events most frequently. In future, the frequency, duration, severity and intensity of compound events increase throughout China in response to anthropogenic climate change, of which the frequency would increase by 1-3 times and the duration and severity increase by 50%, independent of the emission scenarios. The new index can provide a new tool to quantify sub-monthly characteristics of compound dry and hot events, conducive to the timely monitoring of their initiation, development, and decay which are vital for decision-makers and stake-holders to release early and timely warnings.

Keywords: compound event; SCDHI; SAPEI; sub-monthly scale; China

https://doi.org/10.5194/hess-2020-383
Preprint. Discussion started: 28 July 2020


Hydrology and Earth System Sciences
Discussions

1 Introduction

Compound dry and hot event (CDHE) have been observed for all continents in recent decades (Hao et al., 2019; Mazdiyasni and AghaKouchak, 2015; Manning et al., 2019; Sutanto et al., 2020). The frequent CDHEs have led to more devastating impacts on natural ecosystems and human society than individual events (Zscheischler et al., 2014; Chen et al., 2019; Hao et al., 2018a). For example, Russia was simultaneously struck by an unprecedented drought and hot in the summer of 2010, which caused large-scale crop failures, wildfires, and human mortality (Zscheischler et al., 2018). Unfortunately, the extreme droughts and hots are expected to occur more frequently in the coming decades under global warming, which potentially results in more compound events in many parts of the world, especially for wet and humid regions (Wu et al., 2020; Swain et al., 2018, Zscheischler and Seneviratne, 2017a). Therefore, understanding such events are of crucial importance to provide the most fundamental information to help disaster mitigation.

Much effort has been made to study the compound events in recent years. Utilizing different thresholds to define the concurrent climate extremes for a specific period, the frequency of compound events has received a great deal of attention (Wu et al., 2019; Zhang et al., 2019). Although this approach can detect compound event occurrence, it fails to quantitatively measure compound event characteristics such as duration, severity, and intensity, and is inconvenient for comparison of compound event characteristics through different climates (Wu et al., 2020). Therefore, to overcome these shortages, several joint climate extreme indices have been proposed for analyzing the characteristics of the compound events. For example, the climate extreme index integrated by temperature and soil moisture extremes was presented for monitoring trends in multiple types of climate extremes across large regions, and has been

https://doi.org/10.5194/hess-2020-383
Preprint. Discussion started: 28 July 2020


Hydrology and Earth System Sciences
Discussions
Open Access
EGU

66 employed to assess changes in spatial extent (Gallant et al., 2014). In recent years,
67 several compound dry and hot indices have been developed. For example, the
68 Standardized Dry and Hot Index based on the ratio of the marginal probability
69 distribution functions of precipitation and temperature was proposed to measure the
70 extreme degree of a compound drought and hot extreme event (Hao et al., 2018). Hao
71 et al. (2019) recently proposed the Standardized Compound Event Indicator (SCEI) to
72 assess the severity of compound dry and hot events by jointing the marginal distribution
73 of Standardized Precipitation Index (SPI) and Standardized Temperature Index (STI)
74 using the copula theory. These two joint indices provide useful tools to improve our
75 understanding of the frequency, spatial extent and severity of CDHE. However, they
76 are inevitably subjected to some shortcomings including the fixed monthly scale and
77 the disregard of evapotranspiration, which may limit their use in monitoring the detailed
78 evolution of compound dry and hot events.

79 With the occurrence of extreme climate (e.g. high temperature, low humidity, and
80 sunny skies), droughts can evolve rapidly (Chen et al., 2019; Koster et al., 2019; Mo
81 and Lettenmaier, 2015; Otkin et al., 2018; Yuan et al., 2019; Li et al., 2020a). Such
82 extreme weather can appear within a short period without resulting in long-lasting
83 compound events, but rather, short-term droughts and heatwaves lasting a few weeks
84 or even days (Mo and Lettenmaier, 2016; Zhang et al., 2017). Severe concurrent
85 drought and heat can suddenly strike a region with a relatively short duration when
86 extreme weather anomalies persist over the same region (Röthlisberger and Martius,
87 2019; Wang et al., 2016). Concurrent short-term drought and hot can pose greater
88 potential socio-economic risks because the combination of these events can exacerbate
89 their respective environmental and societal impacts (Kirono et al., 2017; Schumacher
90 et al., 2019; Sedlmeier et al., 2018). Specifically, even short-term concurrent dry and

https://doi.org/10.5194/hess-2020-383
Preprint. Discussion started: 28 July 2020


Hydrology and Earth System Sciences
Discussions

hot extremes can lead to significant agricultural loss if they occur within sensitive stages in crop development such as emergence, pollination, and grain filling (Zhang et al., 2019). For example, a strong precipitation deficit along with record high temperatures have led to severe impacts during May and early June in 2012 across the central U.S. (Ford and Labosier, 2017; Otkin et al., 2013). Such short-term concurrent dry and hot events regularly inflict widespread agricultural crop losses and drastically cut down livestock population, making it one of the most costly natural hazards in the U.S. history at tens of billions of economic losses (Anderson et al., 2016; Otkin et al., 2019). Under climate change, short-term concurrent dry and hot extremes are expected to increase (especially for humid regions), potentially causing substantial damage to natural ecosystems and society (Li et al., 2020b; Sun et al., 2019). To improve understanding of such short-term compound events and make early and timely warnings, decision-makers and stakeholders require more detailed information such as the start time, severity, and the projected tendency in the coming days rather than the average state at a fixed monthly scale. Correspondingly, sub-monthly scale indices for characterizing short-term compound dry and hot events are needed. Through the influence of evapotranspiration, short-term meteorological variables (e.g., solar radiation and sunshine duration) are considered an important factor in drought and heatwave concurrences (James et al., 2010). For example, the largely increase in sunshine duration due to clear sky creates excessive evapotranspiration, which in turn decreases soil moisture (Ford et al., 2015). More surface sensible heat fluxes is transferred to the near-surface atmosphere to further increase air temperatures and prohibit precipitation (Miralles et al., 2019; Vogel et al., 2018). Together, these land-atmosphere interactions create favorable conditions for concurrent drought and heatwaves (Mo and Lettenmaier, 2016; Otkin et al., 2018). Thus, the development of a compound drought and heat index

https://doi.org/10.5194/hess-2020-383
Preprint. Discussion started: 28 July 2020


Hydrology and Earth System Sciences
Discussions

should consider other important drought/hot-related factors including temperature and precipitation (e.g. evapotranspiration).

The complexity of compound events makes it an unusual task to develop a simple and robust index to quantify their past and future changes (Zscheischler et al., 2020). A suite of indices are proposed for the assessments of droughts and heatwaves previously, yet there is no index available for incorporating the joint variability of dry and hot conditions at sub-monthly scale. Here we aim to formulate a compound drought and heat index, called the standardized compound drought and heat index (SCDHI), for monitoring and analyzing compound dry and hot events at sub-monthly scale. To achieve this aim, we combine a daily scale drought index, the standardized antecedent precipitation evapotranspiration index (SAPEI), which simultaneously considers precipitation and potential evapotranspiration (PET), with a daily scale standardized temperature index (STI). We investigate the characteristics such as frequency, duration, severity, and intensity of CDHEs during the historical (1961-2018) period and project their changes in China for the future (2050-2100) under different emission scenarios. This index can provide a new tool to quantify the characteristics of CDHEs, and can monitor the CDHE at multiple time scale (e.g., daily, weekly and monthly) to provide detailed information on their initiation, development, decay, and trends.

2 Methods

2.1 data

Daily meteorological datasets covering 1961 to 2018 were collected from 2239 observational stations across the non-arid region in China (Fig. 1), which include precipitation (P), maximum air temperature (T_{max}), mean air temperature (T_{men}), minimum air temperature (T_{min}), relatively humidity (RH), wind speed (WS), and sunshine duration. All of these meteorological data with strict quality control are

https://doi.org/10.5194/hess-2020-383
Preprint. Discussion started: 28 July 2020


Hydrology and Earth System Sciences
Discussions

141 available from the China Meteorological Administration (http://cdc.nmic.cn/home.do)
142 and the Resources and Environmental Science Data Center, Chinese Academy of
143 Sciences (http://www.resdc.cn/Default.aspx). The kriging method was applied to
144 interpolate these observational station data into 0.25× 0.25° gridded data.

145 The two commonly used indices (i.e., monthly Palmer Drought Severity Index
146 (PDSI) and Standardized Precipitation Evapotranspiration Index (SPEI) were employed
147 for comparison. PDSI and SPEI were computed from the same meteorological data
148 described above. The conventional PDSI was empirically derived using the
149 meteorological data of the central USA with its semi-arid climate. The portability of
150 the conventional PDSI is thus relatively poor (Liu et al., 2017). In this study, PDSI was
151 calculated according to the China national standard of classification of meteorological
152 drought with standard number of GB/T 20481-2017. The PDSI calculation procedure
153 of this standard was built based on long-term meteorological data of in-situ stations
154 evenly distributed around China, hence well monitor drought in China (Zhong et al.,
155 2019a). The 0.25°-daily root zone (0 - 100 cm) soil moisture dataset obtained from
156 Community Land Model (CLM) of the Global Land Data Assimilation System
157 (GLDAS) was also used in this study. The dataset from 1961 to 2014 were downloaded
158 from the Goddard Earth Sciences Data and Information Services Center (Rodell et al.,
159 2004). The GLDAS CLM soil moisture dataset captures dry and wet conditions in
160 China well (Bi et al., 2016; Feng et al., 2016). In addition, 8-day leaf area index (LAI)
161 of the MOD15A2H from 2003 to 2018 were collected. These data were resampled to
162 0.25° spatial resolution, and then the Z-score was used to calculate the LAI anomalies.

163 We further used eight global climate models from the Coupled Model
164 Intercomparison Project Phase (https://esgf.llnl.gov/) (Taylor et al., 2012), including
165 CanESM2, CNRM-CM5, CSIRO-Mk3.6, MIROC-ESM, MPI-ESM-LR, BCC-CSM1-

https://doi.org/10.5194/hess-2020-383
Preprint. Discussion started: 28 July 2020


Hydrology and Earth System Sciences
Discussions

1, IPSL-CM5A-LR, and MRI-CGCM3, were used to project the future climate conditions. These GCMs exhibit good performance to simulate the key features of precipitation and temperature in China (Jiang et al., 2016; Yang et al., 2019). We obtained daily climate variables (i.e., P, T_{max}, T_{min}, T_{men}, WS, RH, and shortwave and longwave radiations) for the historical (1961-2005) and future (2030-2100) periods for the three Representative Concentration Pathways (RCPs) including RCP 2.6 (low emission scenario), RCP 4.5 (moderate emission scenario) and RCP 8.5 (high emission scenario). All of the GCM outputs were based on the first ensemble member of each model, referred to as *r1i1p1* in all of the experiments. The detailed information on these GCMs is shown in Table S1.

2.2 Development of SCDHI

The SCDHI is a compound drought and heat index based on a daily drought index and the Standardized Temperature Index (STI), which is computed in a similar fashion as the Standardized Precipitation Index (Zscheischler et al., 2014). The calculation of daily STI is similar to monthly STI, but for standardizing daily temperature. For example, with respect to one certain grid point, the 1 January STI are computed on the 1 January temperature datasets observed during 1961-2018 at each grid point. We firstly formulated a daily scale drought index, i.e. the standardized antecedent precipitation evapotranspiration index (SAPEI), by considering both precipitation and PET. Afterward, the joint distribution method was employed to compute the SCDHI.

2.2.1 Formulation of daily-scale drought index

Li et al. (2020b) have proposed the daily-scale drought index (SAPEI) that considers both precipitation and PET. However, the primary limitation of this index is that it has a fixed temporal scale and cannot reflect the dry and wet condition at different time scales. Hence, in this study, we developed the multiple time scale (i.e., 3-, 6-, 9-,

https://doi.org/10.5194/hess-2020-383
Preprint. Discussion started: 28 July 2020


Hydrology and Earth System Sciences
Discussions

and 12-month) daily drought index. Here, we followed the same nomenclature proposed by Li et al. (2020b) to refer to a daily standardized drought index (SAPEI) based on precipitation and PET. SAPEI is simple to calculate, and uses the antecedent accumulative differences between precipitation and PET to represent the dry and wet condition of the current day. The calculation procedure is described below.

The Penman-Monteith method (Allen et al., 1998) was firstly used to compute PET. With a value for PET, the daily difference between precipitation and PET was calculated to reveal climatic water balance (precipitation minus PET). To reflect dry and wet conditions of the day, the antecedent water surplus or deficit (D) was calculated through the following equations:

$$D = \sum_{i=1}^{n} \left(p - PET \right)_i \quad (1)$$

Where n is the number of previous days.

The D values can be aggregated at different time scales, such as 3, 6, 9 months, and so on. A probability distribution was used to fit the daily time series of D. Given that different probability distributions may cause differences in drought indices (Stagge et al., 2015), to select the most suitable distribution, several commonly probability distributions including the general extreme value, log-logistic, lognormal, Pearson III, generalized Pareto, exponential, and normal distributions, should be used to fit the D series. In the study of Li et al. (2020b), Shapiro-Wilk and Kolmogorov-Smirnov (KS) test have been used applied for optimal probability distribution selection by comparing the empirical probability distribution with a candidate theoretical probability distribution. They suggested that the log-logistic distribution is more suitable for SAPEI. Moreover, previous researches have demonstrated that the log-logistic distribution is suitable for standardizing drought indices, e.g. SPEI (Vicente-Serrano et

https://doi.org/10.5194/hess-2020-383
Preprint. Discussion started: 28 July 2020


Hydrology and Earth System Sciences
Discussions

al., 2010). Therefore, we chose the log-logistic distribution to compute SAPEI. Once the daily D series were fit to a probability distribution, cumulative probabilities of the D series were obtained and transformed to standardized units (SAPEI) using the classical approach of Barton et al. (1965).

2.2.2 Construction of SCDHI

The SCDHI was established through copula theory, which can combine the candidate variables into one numerical expression. This approach not only realizes a projection from multiple dimensions to a single dimension, but also the marginal distributions of the candidate variables combined with their original structures can be fully preserved within the constructed joint distribution. Hence, the copula-based index provides an objective description of the compound events (Hao et al., 2018b; Terzi et al., 2019).

There are many copula families available, which have widely been used for joint bivariate distributions (Terzi et al., 2019; Zhang et al., 2018). Among then, Clayton, Gumbel, Normal, T, and Frank copula perform well for jointing bivariate hydrometeorological variables (Ayantobo et al., 2018; Liu et al., 2019), and thus were employed to establish the bivariate joint probability distribution in this study. Assuming, the two random Gaussian variables X and Y representing SAPEI and STI, respectively, the CDHE can be identified as one variable X lower than or equal to a threshold x, and the other variable Y higher than a threshold y at the same time. The joint probability p of the CDHE can then be expressed as:

$$p = P(X \le x, Y \ge y) = u - c(u,v) \quad (2)$$

where u was the X marginal distribution, and $c(u,v)$ was the joint probability

https://doi.org/10.5194/hess-2020-383
Preprint. Discussion started: 28 July 2020


Hydrology and Earth System Sciences
Discussions

236 distribution.

237 This joint cumulative probability p could be treated as an indicator, where smaller

238 p values denote more severe condition of CDHE. However, p to the given marginal

239 sets, p values in different seasons or areas reflected different conditions and are thus

240 not comparable. Hence, the joint probability p was transformed to a uniform

241 distribution by fitting a distribution F, which was then standardized as an indicator to

242 characterize CDHEs. Once the p series at each day were fitted to a copula, the p

243 series were transformed to standardized units. SCDHI can be estimated by taking the

244 inverse of joint cumulative probability (p) as:

$$SCDHI = \varphi^{-1}(F(P(X \le x, Y \ge y))) \quad (3)$$

245 where φ is the standard normal distribution function. the distribution F was

246 estimated based on the Yeo-Johnson transformation formula (Yeo and Johnson, 2000).

247 Following the categories of compound dry and hot conditions as suggested by (Wu

248 et al., 2020), we defined five categories of compound dry and hot conditions, including

249 abnormal, light, moderate, heavy and extreme compound drought-hot, as shown in

250 Table 1.

251 We used Akaike information criterion (AIC), Bayesian information Criterion (BIC),

252 and KS statistics as goodness-of-fit measures to select an appropriate copula. These

253 statistical measures have been commonly used for estimating the goodness of fit of a

254 proposed cumulative distribution function to a given empirical distribution function

255 (Liu et al., 2019; Terzi et al., 2019). The AIC, BIC, and KS statistics are presented in

256 Fig. S1-3. According to the evaluation metrics, there was a good agreement between

https://doi.org/10.5194/hess-2020-383
Preprint. Discussion started: 28 July 2020


Hydrology and Earth System Sciences
Discussions

the empirical and parametric copulas. Particularly, the performance of Frank copula slightly outweighed those of the other three copulas. Therefore, the Frank copula was utilized to establish the joint probability function and construct SCDHI in this study. Note that the SCDHI under three future scenarios is also used the Frank copula, while the parameters are assessed by future scenarios data. The SCDHI development was illustrated in Fig. S4.

Furthermore, to verify the ability of SCDHI to capture the compound dry and hot event, three verification metrics were used (i.e., probability of detection (POD), false alarm ratio (FAR), and critical success index (CSI)) (Zhang et al., 2018).

$$POD = H/(H+M) \tag{4}$$

$$FAR = F/(H+F) \tag{5}$$

$$CSI = H/(H+F+M) \tag{6}$$

where H (Hit, observed drought-hot) refers to the number of grids when SAPEI and STI is subjected to grade 1 (G1) - grade 4 (G4) and SCDHI is subjected to G1-G4; M (Miss) denotes the number of grids when SAPEI and STI is between G1 to G4 and SCDHI is subjected to other grades than G1-G4; F (false alarm) denotes the number of grids when SAPEI and STI is subjected to other grades than G1-G4 but SCDHI is subjected to grades of G1-G4.

3 Results and Discussion

3.1 Evaluation of SAPEI

The SCDHI was established based on the STI and daily-scale drought index, i.e., SAPEI. However, no previous studies have tested the (daily) drought monitoring performance of SAPEI. When developing a drought index, rigorous testing is required

https://doi.org/10.5194/hess-2020-383
Preprint. Discussion started: 28 July 2020


Hydrology and Earth System Sciences
Discussions

277 with respect to its applicability before it is applied in drought monitoring. Fig. 2 shows
278 the spatial distributions of the correlations between SAPEI and SPEI/PDSI/soil
279 moisture across China. The monthly mean SAPEI at 3-, 6-, 9- and 12-month scale all
280 showed strong agreement with the SPEI in China, with correlation coefficients higher
281 than 0.8 ($p < 0.01$), indicating that the monthly SAPEI at multiple time scale calculated
282 from the daily value could have the same capability of monthly drought monitoring as
283 SPEI. The 3-, 6-, 9- and 12-month SAPEI generally showed good correlation with PDSI,
284 and 3-month SAPEI and PDSI generally correlate closely, with correlation coefficients
285 higher than 0.6 ($p < 0.01$), while the 12-month SAPEI displayed weak correlation with
286 PDSI in south China. For daily SAPEI at 3-month scale and soil moisture, a close
287 correlation was detected in south China, while relatively weak correlation is found in
288 north China. The correlation between SAPEI and soil moisture increased in magnitude
289 and spatial extent at time scales of 6-12 months. For 12-month SAPEI, correlation
290 coefficient was generally greater than 0.6 for a majority of China. This phenomenon
291 implied that the short-time scale SAPEI was more sensitive to precipitation change, and
292 thus could be more suitable for meteorological drought, while the long-time scale (more
293 than five month) SAPEI was more closely related to soil moisture and can be applied
294 for agricultural drought monitoring. Overall, these analyses indicate that the SAPEI at
295 daily and monthly scale showed reliability in drought monitoring

296 To further test the drought monitoring performance of the SAPEI, typical drought
297 events were chosen as case studies. During recent decades, several well-known large-
298 scale drought events have hit China, including the droughts in winter of 2009 to spring
299 of 2010, and in 2011 (Lu et al., 2014; Yu et al., 2019). In this study, the drought regimes
300 during these events were taken as case studies to evaluate the drought monitoring
301 performance of SAPEI at 3- and 6-month time scales (Sun and Yang, 2012). We firstly

https://doi.org/10.5194/hess-2020-383
Preprint. Discussion started: 28 July 2020


Hydrology and Earth System Sciences
Discussions

showed the monthly evolution of these events by the monthly mean SAPEI, SPEI, and PDSI, and then analyzed the daily evolution of drought in space and time in the most affected areas according to SAPEI and soil moisture.

3.2.1 Drought events during 2009-2010

Fig. S5 illustrates the monthly changes in the 2009/10 drought monitored by the PDSI, SPEI, and SAPEI at 3- and 6-month scale. This drought started to appear in most of China (except for the central and northeast China) in September 2009, and then persisted in most of China during October to December 2009; during this period, drought conditions became more severe in south China. The drought in north and east China gradually faded away during January and March in 2010. In contrast, in southwest China (SWC) the drought intensity became rather strong during the same period. The severe dry condition continued in SWC during April in 2010, while drought in the rest of China gradually disappeared in this period. After that, dry conditions in SWC gradually relieved from May to June in 2010, but did not disappear. The monthly drought evolution based on SAPEI was generally similar with that of SPEI and PDSI.

Despite being located in the humid climate zone, SWC suffered from exceptional drought during the autumn of 2009 to the spring of 2010 (Lin et al., 2015). During this drought, more than 16 million people and 11 million livestock faced drinking water shortages, with direct economic losses estimated at 19 billion yuan in SWC (Lin et al., 2015). We selected this event in SWC as the first case study, and reveal detailed spatial and temporal change of this event at daily scale based on SAPEI and soil moisture (Fig. 3 and 4). During September 1 to 30 of 2009, the drought started to appear in the region, and dry conditions became worse and spread throughout nearly the entire SWC from October 1 to November 15 of 2009. Severe dry conditions then stayed in the region for 152 days from November 15 to April 15 of 2010, with high intensity.

https://doi.org/10.5194/hess-2020-383
Preprint. Discussion started: 28 July 2020


Hydrology and Earth System Sciences
Discussions

Afterwards, severe drought was gradually relieved from April 15 to June 15. The drought diminished over time in most parts of southwest China by the end of June.

3.2.2 Drought events in 2011

The monthly changes in the 2011 drought is illustrated in Fig. S6. The drought pattern monitored by SAPEI generally shows a good agreement with those by SPEI and PDSI. More specifically, the drought mainly started in north China in January, while in March it spread to most of China, and drought conditions in lower reaches of the Yangtze River basin became serious. In April to May, severe dry conditions persisted in the middle and lower reaches of the Yangtze River Basin (MLR-YRB), and extended from the YRB to southern China. In August, the drought moved westward and reached the edge of southwestern China. Severe drought persisted in the region during September and October, but it gradually faded away in November and December. The results monitored by the SAPEI are generally consisted with the findings of Lu et al. (2014).

The 2011 drought event was particularly unusual in the LR-YRB. The MLR-YRB is generally in a wet condition, nevertheless, suffered its worst drought in the 50 years during the spring. The severe drought caused shortage of drinking water for 4.2 million people. 3.7 million hectares of crops were damaged or destroyed. Moreover, the heavy drought led to more than 1,300 lakes devoid of all water in Hubei province (Xu et al., 2015). The temporal and spatial evolution of this event in MLR-YRB described by daily SAPEI and soil moisture was shown in Fig. 5-6. The drought started to appear in the north part of the MLR-YRB in early February of 2011, and then gradually expanded to the whole MLR-YRB during early February and March 15. The severe drought condition persisted in this region for 78 days (from March 15 to May 31). Afterwards, there was a tendency toward alleviating drought conditions, and most of MLR-YRB

https://doi.org/10.5194/hess-2020-383
Preprint. Discussion started: 28 July 2020


Hydrology and Earth System Sciences
Discussions

was under light and moderate drought conditions.

The previous detailed analysis showed that the SAPEI not only captures monthly characteristics of droughts, but also has the potential to track droughts at sub-monthly scale. Though the input data (including precipitation and PET) of SAPEI are similar to SPEI, the rationale of the index is different from SPEI. It was calculated for each day and considers the water surplus or deficit of that day and the previous days. SPEI was commonly employed to monitor and analyze the monthly or longer-scale droughts (Vicente-Serrano et al., 2010). It thus may not be appropriate to apply the SPEI at shorter timescales (e.g., daily or weekly), because of the inherent problem in the construction of the index. Although SPEI gives a full and equal consideration to the water surplus or deficit in the period of the considered time scale, it does not consider the water surplus or deficit in the days before the period. If the scale is very short, this may cause problems. For a 7-day period, for example, if there is no precipitation during the period, it may be regarded as a drought period when compared with historical records (the method used by the SPEI); however, if there is a heavy precipitation just before the period, then the 7-day period probably remains wet and is unlikely to experience drought condition during such a short time. Previous studies have demonstrated the disadvantage of SPEI for short-time scale drought monitoring (Lu, 2009; Lu et al., 2014; Li et al., 2020b).

In summary, the SAPEI meets the requirements of a drought index, given the fact that it shows reliable and robust ability for drought analysis and monitoring. Like the SPEI, SAPEI includes multiple time scales (3-, 6-, 9-, and 12- month) to monitor droughts at monthly resolution. However, SAPEI has the advantage over SPEI regarding sub-monthly drought monitoring.

https://doi.org/10.5194/hess-2020-383
Preprint. Discussion started: 28 July 2020


Hydrology and Earth System Sciences
Discussions
Open Access
EGU

3.2 Evaluation of SCDHI

The SCDHI was developed by joining the marginal distribution of the SAPEI and STI. Though the copula method has been widely utilized to connect bivariate distribution, the property of SCDHI in capturing CDHEs still needs to be tested. Fig. 7 shows the spatial distributions of the correlations between SCDHI and SAPEI/STI at daily scale across China. The SCDHI all showed strong ($p < 0.01$) correlation with the SAPEI at 3-, 6-, 9- and 12-month scale in China, with correlation coefficients higher than 0.7. A significant correlation ($p < 0.01$) was also detected between STI and SCDHI at multiple scales. Fig. 8 shows the spatial pattern in POD, FAR, and CSI when the drought and hot events observed by SAPEI and STI, respectively, were related to compound drought-hot event detected by SCDHI at 3-, 6-, 9- and 12-monthly scale. As shown in Fig. 8, POD is close to 1 and FAR is close to 0, implying that SCDHI can well detect in most of the areas where the droughts and hots were detected by SAPEI and STI. The values of CSI indicated that the ratios of drought-hot affected areas detected by SAPEI and STI to the drought and hot areas detected by SCDHI were close to one. Overall, these analyses implied that SCDHI can well monitor droughts and hots that can be successfully captured by SAPEI and STI. The SCDHI thus detects CDHEs that are identified separately by the coincidence of low SAPEI and high STI. In addition, the SCDHI detects events that are very extreme in either the SAPEI or the STI and moderate in the other variable but thus still cause substantial damage (Zscheischler et al., 2017b). Furthermore, the SCDHI is able to quantify the magnitude of CDHEs.

To further test the drought-heat monitoring performance of the SCDHI, two typical CDHEs were chosen as case studies according to the Yearbook of Meteorological Disasters in China. One was a well-known compound drought and heatwave striking Sichuan-Chongqing region (SCR) with serious consequences during summer of 2006

https://doi.org/10.5194/hess-2020-383
Preprint. Discussion started: 28 July 2020


Hydrology and Earth System Sciences
Discussions

(Wu et al., 2020), and the other occurred in southern China with adverse impacts on agriculture during July to September of 2009 (Wang et al., 2010). SCR experienced continuous extreme temperature during mid-June to late August 2006. The duration and severity of this hot event were the worst on the historical record. Simultaneously, a heavy drought occurring once in 100 years hit this region. During this compound event, a population of over ten million was confronted with drinking water shortage, about twenty thousand km^2 of cropland suffered serious losses, and more than one hundred times forest fire broke out. Local governments issued the most serious arid warning (Zhang et al., 2008). Thus, we take this typical drought-hot event as first case studies to evaluate the drought/hot monitoring performance of SCDHI. The monthly spatial pattern of this compound event in SCR is shown in Fig. S7, indicating that SCR during summer in 2006 experienced the moderate to extreme compound dry and hot conditions. Fig. 9 maps the spatial pattern of this compound event and its impact on vegetation from mid-June to late August. This event started to appear in SCR in mid-June 2006, and gradually spread throughout the whole SCR during June 19 to 26. The moderate dry-hot condition then persisted in the entire SCR from June 27 to August 5 in 2006, lasting for 40 days. The negative LAI was scattered in some of the dry-hot affected areas. However, during August 6 to 21, the drought-hot event became even more severe with the onset of extremely hot temperatures, causing negative vegetation anomalies in most of the affected areas.

The monthly spatial pattern of another compound event in southern China during July to September of 2009 is shown in Fig. S8. Overall moderate to heavy compound dry and hot conditions are observed at monthly scale in this region. However, this event showed large fluctuation at weekly scale. According to the Yearbook, the hot event was divided into two periods: the first stage was from early to late July, and the other stage

https://doi.org/10.5194/hess-2020-383
Preprint. Discussion started: 28 July 2020


Hydrology and Earth System Sciences
Discussions

was from mid-August to early September. The fluctuating compound event caused adverse impact of crop pollination and grain filling, resulting in decrease of crop production. Fig. 10 maps the spatial pattern of this event and its impact on LAI. In the first stage, the drought-hot event hit the most of southern China during July 5 to 12, and then it became severe in the west part of southern China during July 13 to 20. However, the hot event suddenly disappeared from July 21 to 28, leading to disappearance of the compound event in most of southern China (Fig. 10a). Afterward, the compound event hit this region again from August 6 to 13, and its intensity was strong during August 14 to 21, with severe hot conditions. Subsequently, the intensity and spatial extent of the compound event faded away in north of southern China during August 22 to 29. This event extended to most of this region again from August 30 to September 14, with severe dry and hot condition. The compound events still stayed in this region from September 15 to 22 (Fig. 10b). Despite the short-term event, the anormal change in vegetation was found in most of the dry-hot affected areas. This complex event indicates that monthly analyses of the event can provide an overall situation, but is not be able to capture the serious dry and hot conditions caused by a short-term extreme climate anomaly at shorter time scales. Though such short-term compound event only lasted for days or weeks, they lead to large agricultural losses if they occur within sensitive stages in crop development (i.e., pollination and grain filling) (Mazdiyasni and AghaKouchak, 2015). To provide timely information of the CDHEs, short-time scale analyses and monitoring of such events are essential.

Overall, the changes in these two CDHEs based on SCDHI are consistent with the national weather reports (http://www.weather.com.cn/). In summary, the SCDHI is able to robustly and reliably capture CDHEs at sub-monthly scale, and potentially provide a new tool to objectively and quantitatively analyze and monitor the characteristics of

https://doi.org/10.5194/hess-2020-383
Preprint. Discussion started: 28 July 2020

451 CDHEs in time and space.

452 **3.3 Application**

453 Here, we evaluate and compare the spatiotemporal variation of characteristics of
454 CDHEs in China. More precisely, the CDHEs during growing season (April-September)
455 from 1961 to 2018 were identified based on 3-month scale SCDHI and run theory (Wu
456 et al., 2018), after which the frequency, duration, severity, and intensity of these events
457 were analyzed (A specific case to identify CDHE is shown in Fig. S9). We then
458 projected their future characteristics changes under the RCP 2.6, 4.5 and 8.5 from 2050
459 to 2100. Given that short-term concurrent dry and hot events generally persist for at
460 least weeks (Otkin et al., 2018), only the events lasting for more than two weeks were
461 considered in this study.

462 Fig. 11 shows spatial patterns of characteristics of the CDHEs. A high frequency of
463 compound events was detected in southern China, with occurrence of every two years
464 on average, in contrast, the eastern Tibet Plateau and northeast China experienced fewer
465 compound events (Fig. 11a), which was generally consistent with the previous studies
466 (Liu et al., 2020; Wang et al., 2016). The CDHE generally lasted for about twenty-five
467 to thirty-five days in most of China, while in east Tibet Plateau, the CDHE persisted
468 for less than twenty days (Fig. 11b). The severity and intensity of the CDHE presented
469 relatively similar patterns and showed that most of eastern China experienced high
470 severity and intensity (Fig. 11 c-d). Overall, southern China suffered more frequent
471 CDHEs, with higher severity and intensity. Southern China is a humid region where
472 evapotranspiration is mainly controlled by energy supply because soil moisture is
473 usually sufficient. For given adequate soil moisture in the initiation of drought,
474 evaporative demand can increase rapidly during a short period when strong, transient
475 meteorological changes (such as extreme temperature) occur, which in turn exhaust soil

https://doi.org/10.5194/hess-2020-383
Preprint. Discussion started: 28 July 2020


Hydrology and Earth System Sciences
Discussions

476 moisture to intensify drought conditions (Zhang et al., 2019, Otkin et al, 2018).
477 Moreover, vegetation over south China is usually abundant and plants tend to suck more
478 water from the soil when high temperatures occur, causing evapotranspiration increase
479 and soil moisture decline (Li et al., 2020c; Wang et al., 2016). More surface sensible
480 heat fluxes are thus transferred to the near-surface atmosphere to further increase air
481 temperatures (Mo and Lettenmaier, 2015). These land-atmosphere interactions
482 altogether cause the Bowen ratio to increase (Otkin et al., 2013, 2018), creating a
483 favorable condition for short-term concurrence droughts and hots. Therefore, CDHEs
484 are more likely to occur in humid regions with higher severity and intensity.

485 Fig. 12 illustrates the spatial patterns of change in frequency, duration, severity, and
486 intensity of the CDHEs under RCP 2.6, 4.5, and 8.5 scenarios. According to Fig. 12a,
487 the future (2050-2100) CDHE frequency under three scenarios in most of east China
488 will increase by about one to three times with respect to the reference period (1961-
489 2018). Under RCP 8.5 scenario, CDHE at about 4% of the study region is expected to
490 markedly increase by more than five times, which are scattered in the central to west
491 parts of China. The duration of CDHE across the east of the study region will mainly
492 show an increase of about 0.5 times, while duration in mid-west China potentially
493 increases by approximately 1.5 times under RCP 8.5 scenarios (Fig. 12b). The spatial
494 pattern of future severity change is similar to the duration; severity in most of east China
495 is projected to increase by about 0.5 time under three scenarios; however, CDHE
496 severity over mid-west China is expected to more than triple under RCP 8.5 (Fig. 12c).
497 The CDHE intensity in most of the study region exhibits slight increase for all scenarios
498 in comparison to the historical period.

499 The cumulative density functions (CDFs) of the CHDE frequency, duration,
500 severity, and intensity in historical and future periods were quantified, and the result is

https://doi.org/10.5194/hess-2020-383
Preprint. Discussion started: 28 July 2020


Hydrology and Earth System Sciences
Discussions
Open Access
EGU

501 shown in Fig. 13. A substantial change in the values of CHDE frequency, duration,
502 severity, and intensity was detected between the historical and future projections. The
503 frequency, duration, severity, and intensity of CHDEs will intensify throughout the
504 China in future scenarios compared to the historical reference, as marked by the
505 movement towards the right side of the CDF curves. Specifically, the cumulative
506 probability of CDHE frequency is expected to increase by more than 80% under three
507 scenarios, compared with the 95th percentile value in historical period (Fig. 13a). The
508 cumulative probability of duration would increase by about 72% under RCP 8.5
509 scenario, while increment under RCP 2.6 scenario is relatively small (17%), in
510 comparison to the 95th percentile in reference period (Fig. 13b). The severity cumulative
511 probability project to increase by 42% and 53% under RCP 2.6 and 4.5 scenarios
512 respectively, but even increase by 88% under RCP 8.5 scenario (Fig. 13c). An increase
513 of at least 42% is observed in the intensity cumulative probability, compared with the
514 n reference period (Fig. 13d). Such an increase in the frequency, duration, severity, and
515 intensity of CDHEs across China could be a new normal in future.

516 Global warming is very likely to exacerbate the prevalence of the CDHEs
517 (Pfleiderer et al., 2019). Trends are often present in individual variables (e.g.,
518 temperature, and precipitation), while can also occur in the dependence between drivers
519 of compound events, which consequently affects associated risks. The (negative)
520 correlation between seasonal mean summer temperature and precipitation is projected
521 to intensify in many land regions, leading to more frequent extremely dry and hot
522 conditions (Kirono et al., 2017; Zscheischler and Seneviratne, 2017a). Overall, the
523 frequency, severity, duration, and intensity of the CDHEs in China under global
524 warming will increase significantly. Effective measures need to be implemented to
525 decrease the CO^2 emissions for compound dry and hot event mitigation.

https://doi.org/10.5194/hess-2020-383
Preprint. Discussion started: 28 July 2020


Hydrology and Earth System Sciences
Discussions

4 Conclusions

Under global warming, the compound dry and hot event tends to more frequent and short-lived (i.e., days or weeks). Correspondingly, a compound drought and heat index should be able to monitor such event at sub-monthly scales in order to timely reflect dry and hot condition evolution. In this study, we developed a multiple time scale (e.g., 3-, 6-, 9, and 12- month) compound drought and heat index, termed as SCDHI, to monitor short-time (e.g., days or weeks) and long-time (e.g., months) compound event. This index was established based on the daily drought index (i.e., SAPEI) and Standardized Temperature Index (STI) using a joint probability distribution method. Using the SCDHI, we then quantitively investigated the characteristics (i.e., frequency, intensity, severity, and duration) of the CDHEs in China in historical period (1961-2018), and revealed how they would change in the future (2050-2100) under representative concentration pathway (RCP) 2.6, 4.5, and 8.5 scenarios. The main conclusions of this study are presented as follows: The SCDHI can well monitor simultaneous dries and hots detected by SAPEI and STI. The monthly SCDHI can provide an overall situation of the compound dry and hot conditions, but sub-monthly SCDHI can well capture fluctuation of simultaneous dries and hots within a month. It also can reflect the impact of the compound dry and hot event on vegetation anomalies. The SCDHI can offer a new tool to quantitatively measure the characteristics of the CDHEs. It also can provide detailed information such as the initiation, development, decay, and tendency of the compound event for decision-makers and stakeholders to make early and timely warning. In the case study of the China, the southern China suffered more frequent the CDHE, with higher severity and intensity. The CDHE mainly lasted for twenty-five to thirty-five days in China. The frequency, duration, severity, and intensity of compound events will intensify throughout the China in future.

https://doi.org/10.5194/hess-2020-383
Preprint. Discussion started: 28 July 2020


Hydrology and Earth System Sciences
Discussions

551 The frequency will increase by about one to three times with respect to the reference
552 period. A region with fewer compound event (< 5) would exhibit a multi-fold (more
553 than five times) increase in the future. The duration across east areas mainly increased
554 by 0.5 times, while severity project to increase by about 0.5 to 1 times.

555

556 **Data availability.** The observed meteorological datasets are available at
557 http://cdc.nmic.cn/home.do. The CMIP5 datasets are available at https://esgf.llnl.gov.

558

559 **Author Contributions.** Conceived and designed the experiments: JL, WS. Performed
560 the experiments: JL, WS. Analyzed the data: JL. Wrote and edited the paper: JL, WS,
561 WZ, ZJ, GS, CX.

562

563 **Competing interests.** The authors declare that they have no conflict of interest.

564

565 ## Acknowledgement

566 The research is financially supported by the National Natural Science Foundation
567 of China (51879107, 51709117), the Guangdong Basic and Applied Basic Research
568 Foundation (2019A1515111144), and the Water Resource Science and Technology
569 Innovation Program of Guangdong Province (2020-29).

570
571
572
573
574
575
576
577
578

https://doi.org/10.5194/hess-2020-383
Preprint. Discussion started: 28 July 2020


Hydrology and Earth System Sciences
Discussions

References

Allen, R. G., Pereira, L. S., Raes, D. and Smith, M.: Crop evapotranspiration: Guidelines for computing crop requirements, Irrig. Drain. Pap. No. 56, FAO, doi:10.1016/j.eja.2010.12.001, 1998.

Anderson, M. C., Zolin, C. A., Sentelhas, P. C., Hain, C. R., Semmens, K., Tugrul Yilmaz, M., Gao, F., Otkin, J. A. and Tetrault, R.: The Evaporative Stress Index as an indicator of agricultural drought in Brazil: An assessment based on crop yield impacts, Remote Sens. Environ., doi:10.1016/j.rse.2015.11.034, 2016.

Ayantobo, O. O., Li, Y., Song, S., Javed, T. and Yao, N.: Probabilistic modelling of drought events in China via 2-dimensional joint copula, J. Hydrol., 559, 373–391, doi:10.1016/j.jhydrol.2018.02.022, 2018.

Barton, D. E., Abramovitz, M. and Stegun, I. A.: Handbook of Mathematical Functions with Formulas, Graphs and Mathematical Tables., J. R. Stat. Soc. Ser. A, doi:10.2307/2343473, 1965.

Bi, H., Ma, J., Zheng, W. and Zeng, J.: Comparison of soil moisture in GLDAS model simulations and in situ observations over the Tibetan Plateau, J. Geophys. Res., doi:10.1002/2015JD024131, 2016.

Chen, L., Chen, X., Cheng, L., Zhou, P. and Liu, Z.: Compound hot droughts over China: Identification, risk patterns and variations, Atmos. Res., 227(May), 210–219, doi:10.1016/j.atmosres.2019.05.009, 2019.

Feng, X., Fu, B., Piao, S., Wang, S., Ciais, P., Zeng, Z., Lü, Y., Zeng, Y., Li, Y., Jiang, X. and Wu, B.: Revegetation in China's Loess Plateau is approaching sustainable water resource limits, Nat. Clim. Chang., doi:10.1038/nclimate3092, 2016.

Ford, T. W. and Labosier, C. F.: Meteorological conditions associated with the onset of flash drought in the Eastern United States, Agric. For. Meteorol.,

https://doi.org/10.5194/hess-2020-383
Preprint. Discussion started: 28 July 2020

doi:10.1016/j.agrformet.2017.08.031, 2017.

Ford, T. W., McRoberts, D. B., Quiring, S. M. and Hall, R. E.: On the utility of in situ soil moisture observations for flash drought early warning in Oklahoma, USA, Geophys. Res. Lett., doi:10.1002/2015GL066600, 2015.

Gallant, A. J. E., Karoly, D. J. and Gleason, K. L.: Consistent trends in a modified climate extremes index in the United States, Europe, and Australia, J. Clim., 27(4), 1379–1394, doi:10.1175/JCLI-D-12-00783.1, 2014.

Hao, Z., Hao, F., Singh, V. P., Xia, Y., Shi, C. and Zhang, X.: A multivariate approach for statistical assessments of compound extremes, J. Hydrol., 565, 87–94, doi:10.1016/j.jhydrol.2018.08.025, 2018a.

Hao, Z., Hao, F., Singh, V. P. and Zhang, X.: Quantifying the relationship between compound dry and hot events and El Niño–southern Oscillation (ENSO) at the global scale, J. Hydrol., 567, 332–338, doi:10.1016/j.jhydrol.2018.10.022, 2018b.

Hao, Z., Hao, F., Singh, V. P. and Zhang, X.: Statistical prediction of the severity of compound dry-hot events based on El Niño-Southern Oscillation, J. Hydrol., 572(February), 243–250, doi:10.1016/j.jhydrol.2019.03.001, 2019.

James, S., Complex, B., Black, S. J., Health, O. and Ando, H.: The synergy between drought and extremely hot summers in the Mediterranean, Biochem. J., 2010.

Jiang, D., Tian, Z. and Lang, X.: Reliability of climate models for China through the IPCC Third to Fifth Assessment Reports, Int. J. Climatol., doi:10.1002/joc.4406, 2016.

Kirono, D. G. C., Hennessy, K. J. and Grose, M. R.: Increasing risk of months with low rainfall and high temperature in southeast Australia for the past 150 years, Clim. Risk Manag., doi:10.1016/j.crm.2017.04.001, 2017.

Koster, R. D., Schubert, S. D., Wang, H., Mahanama, S. P. and Deangelis, A. M.: Flash

https://doi.org/10.5194/hess-2020-383
Preprint. Discussion started: 28 July 2020


Hydrology and Earth System Sciences
Discussions

drought as captured by reanalysis data: Disentangling the contributions of precipitation deficit and excess evapotranspiration, J. Hydrometeorol., doi:10.1175/JHM-D-18-0242.1, 2019.

Li, J., Wang, Z., Wu, X., Chen, J., Guo, S., and Zhang, Z.: A new framework for tracking flash drought events in space and time. Catena, 194, 104763, 2020a.

Li, J., Wang, Z., Wu, X., Xu, C.-Y., Guo, S. and Chen, X.: Toward Monitoring Short-Term Droughts Using a Novel Daily-Scale, Standardized Antecedent Precipitation Evapotranspiration Index, J. Hydrometeorol., 891–908, doi:10.1175/jhm-d-19-0298.1, 2020b.

Li, J., Wang, Z., Wu, X., Guo, S., and Chen, X.: Flash droughts in the Pearl River Basin, China: Observed characteristics and future changes. Sci. Total Environ., 707, 136074, 2020c.

Lin, W., Wen, C., Wen, Z. and Gang, H.: Drought in Southwest China: A Review, Atmos. Ocean. Sci. Lett., 8(6), 339–344, doi:10.3878/AOSL20150043, 2015.

Liu, Y., Zhu, Y., Ren, L., Singh, V. P., Yang, X. and Yuan, F.: A multiscalar Palmer drought severity index, Geophys. Res. Lett., 44(13), 6850–6858, doi:10.1002/2017GL073871, 2017.

Liu, Y., Zhu, Y., Ren, L., Yong, B., Singh, V. P., Yuan, F., Jiang, S. and Yang, X.: On the mechanisms of two composite methods for construction of multivariate drought indices, Sci. Total Environ., 647, 981–991, doi:10.1016/j.scitotenv.2018.07.273, 2019.

Liu, Y., Zhu, Y., Zhang, L., Ren, L., Yuan, F., Yang, X. and Jiang, S.: Flash droughts characterization over China: From a perspective of the rapid intensification rate, Sci. Total Environ., doi:10.1016/j.scitotenv.2019.135373, 2020.

Lu, E.: Determining the start, duration, and strength of flood and drought with daily

https://doi.org/10.5194/hess-2020-383
Preprint. Discussion started: 28 July 2020


Hydrology and Earth System Sciences
Discussions

precipitation: Rationale, Geophys. Res. Lett., 36(12), 1–5, doi:10.1029/2009GL038817, 2009.

Lu, E., Cai, W., Jiang, Z., Zhang, Q., Zhang, C., Higgins, R. W. and Halpert, M. S.: The day-to-day monitoring of the 2011 severe drought in China, Clim. Dyn., 43(1–2), 1–9, doi:10.1007/s00382-013-1987-2, 2014.

Mo, K. C. and Lettenmaier, D. P.: Heat wave flash droughts in decline, Geophys. Res. Lett., doi:10.1002/2015GL064018, 2015.

Mo, K. C. and Lettenmaier, D. P.: Precipitation deficit flash droughts over the United States, J. Hydrometeorol., doi:10.1175/JHM-D-15-0158.1, 2016.

Mazdiyasni, O. and AghaKouchak, A.: Substantial increase in concurrent droughts and heatwaves in the United States, Proc. Natl. Acad. Sci. U. S. A., 112(37), 11484–11489, doi:10.1073/pnas.1422945112, 2015.

Miralles, D. G., Gentine, P., Seneviratne, S. I. and Teuling, A. J.: Land–atmospheric feedbacks during droughts and heatwaves: state of the science and current challenges, Ann. N. Y. Acad. Sci., 1436(1), 19–35, doi:10.1111/nyas.13912, 2019.

Manning, C., Widmann, M., Bevacqua, E., Van Loon, A. F., Maraun, D. and Vrac, M: Increased probability of compound long-duration dry and hot events in Europe during summer (1950-2013). Environmental Research Letters, 14(9), 094006, 2019.

Otkin, J. A., Anderson, M. C., Hain, C., Mladenova, I. E., Basara, J. B. and Svoboda, M.: Examining rapid onset drought development using the thermal infrared-based evaporative stress index, J. Hydrometeorol., doi:10.1175/JHM-D-12-0144.1, 2013.

Otkin, J. A., Svoboda, M., Hunt, E. D., Ford, T. W., Anderson, M. C., Hain, C. and Basara, J. B.: Flash droughts: A review and assessment of the challenges imposed by rapid-onset droughts in the United States, Bull. Am. Meteorol. Soc., 99(5),

https://doi.org/10.5194/hess-2020-383
Preprint. Discussion started: 28 July 2020


Hydrology and Earth System Sciences
Discussions

911–919, doi:10.1175/BAMS-D-17-0149.1, 2018.

Otkin, J. A., Zhong, Y., Hunt, E. D., Basara, J., Svoboda, M., Anderson, M. C. and Hain, C.: Assessing the evolution of soil moisture and vegetation conditions during a flash drought-flash recovery sequence over the South-Central United States, J. Hydrometeorol., doi:10.1175/JHM-D-18-0171.1, 2019.

Pfleiderer, P., Schleussner, C. F., Kornhuber, K. and Coumou, D.: Summer weather becomes more persistent in a 2 °C world, Nat. Clim. Chang., 9(9), 666–671, doi:10.1038/s41558-019-0555-0, 2019.

Rodell, M., Houser, P. R., Jambor, U., Gottschalck, J., Mitchell, K., Meng, C. J., Arsenault, K., Cosgrove, B., Radakovich, J., Bosilovich, M., Entin, J. K., Walker, J. P., Lohmann, D. and Toll, D.: The Global Land Data Assimilation System, Bull. Am. Meteorol. Soc., doi:10.1175/BAMS-85-3-381, 2004.

Röthlisberger, M. and Martius, O.: Quantifying the Local Effect of Northern Hemisphere Atmospheric Blocks on the Persistence of Summer Hot and Dry Spells, Geophys. Res. Lett., doi:10.1029/2019GL083745, 2019.

Schumacher, D. L., Keune, J., van Heerwaarden, C. C., Vilà-Guerau de Arellano, J., Teuling, A. J. and Miralles, D. G.: Amplification of mega-heatwaves through heat torrents fuelled by upwind drought, Nat. Geosci., 12(9), 712–717, doi:10.1038/s41561-019-0431-6, 2019.

Sedlmeier, K., Feldmann, H. and Schädler, G.: Compound summer temperature and precipitation extremes over central Europe, Theor. Appl. Climatol., doi:10.1007/s00704-017-2061-5, 2018.

Stagge, J. H., Tallaksen, L. M., Gudmundsson, L., Van Loon, A. F. and Stahl, K.: Candidate Distributions for Climatological Drought Indices (SPI and SPEI), Int. J. Climatol., doi:10.1002/joc.4267, 2015.

https://doi.org/10.5194/hess-2020-383
Preprint. Discussion started: 28 July 2020


Hydrology and Earth System Sciences
Discussions

704 Sun, C. and Yang, S.: Persistent severe drought in southern China during winter-spring
705 2011: Large-scale circulation patterns and possible impacting factors, J. Geophys.
706 Res. Atmos., doi:10.1029/2012JD017500, 2012.
707 Sun, C. X., Huang, G. H., Fan, Y., Zhou, X., Lu, C. and Wang, X. Q.: Drought
708 Occurring With Hot Extremes: Changes Under Future Climate Change on Loess
709 Plateau, China, Earth's Futur., 7(6), 587–604, doi:10.1029/2018EF001103, 2019.
710 Swain, D. L., Langenbrunner, B., Neelin, J. D. and Hall, A.: Increasing precipitation
711 volatility in twenty-first-century California, Nat. Clim. Chang., 8(5), 427–433,
712 doi:10.1038/s41558-018-0140-y, 2018.
713 Taylor, K. E., Stouffer, R. J. and Meehl, G. A.: An overview of CMIP5 and the
714 experiment design, Bull. Am. Meteorol. Soc., doi:10.1175/BAMS-D-11-00094.1,
715 2012.
716 Terzi, S., Torresan, S., Schneiderbauer, S., Critto, A., Zebisch, M. and Marcomini, A.:
717 Multi-risk assessment in mountain regions: A review of modelling approaches for
718 climate change adaptation, J. Environ. Manage., 232(September 2018), 759–771,
719 doi:10.1016/j.jenvman.2018.11.100, 2019.
720 Vicente-Serrano, S. M., Beguería, S. and López-Moreno, J. I.: A multiscalar drought
721 index sensitive to global warming: The standardized precipitation
722 evapotranspiration index, J. Clim., 23(7), 1696–1718,
723 doi:10.1175/2009JCLI2909.1, 2010.
724 Wang, L., Yuan, X., Xie, Z., Wu, P. and Li, Y.: Increasing flash droughts over China
725 during the recent global warming hiatus, Sci. Rep., doi:10.1038/srep30571, 2016.
726 Wang, W., Wang, W. J., Li, J. S., Wu, H., Xu, C. and Liu, T.: The impact of sustained
727 drought on vegetation ecosystem in southwest China based on remote sensing, in
728 Procedia Environmental Sciences., 2010.

https://doi.org/10.5194/hess-2020-383
Preprint. Discussion started: 28 July 2020


Hydrology and Earth System Sciences
Discussions

729 Wu, J., Chen, X., Yao, H., Liu, Z. and Zhang, D.: Hydrological Drought Instantaneous
730 Propagation Speed Based on the Variable Motion Relationship of Speed-Time
731 Process, Water Resour. Res., doi:10.1029/2018WR023120, 2018.
732 Wu, X., Hao, Z., Hao, F. and Zhang, X.: Variations of compound precipitation and
733 temperature extremes in China during 1961–2014, Sci. Total Environ., 663, 731–
734 737, doi:10.1016/j.scitotenv.2019.01.366, 2019.
735 Wu, X., Hao, Z., Zhang, X., Li, C. and Hao, F.: Evaluation of severity changes of
736 compound dry and hot events in China based on a multivariate multi-index
737 approach, J. Hydrol., 583, 124580, doi:10.1016/j.jhydrol.2020.124580, 2020.
738 Xu, C., McDowell, N. G., Fisher, R. A., Wei, L., Sevanto, S., Christoffersen, B. O.,
739 Weng, E. and Middleton, R. S.: Increasing impacts of extreme droughts on
740 vegetation productivity under climate change, Nat. Clim. Chang., 9(12), 948–953,
741 doi:10.1038/s41558-019-0630-6, 2019.
742 Xu, K., Yang, D., Yang, H., Li, Z., Qin, Y. and Shen, Y.: Spatio-temporal variation of
743 drought in China during 1961-2012: A climatic perspective, J. Hydrol.,
744 doi:10.1016/j.jhydrol.2014.09.047, 2015.
745 Yang, Y., Bai, L., Wang, B., Wu, J. and Fu, S.: Reliability of the global climate models
746 during 1961–1999 in arid and semiarid regions of China, Sci. Total Environ.,
747 doi:10.1016/j.scitotenv.2019.02.188, 2019.
748 Yeo, I. N. K. and Johnson, R. A.: A new family of power transformations to improve
749 normality or symmetry, Biometrika, 87(4), 954–959,
750 doi:10.1093/biomet/87.4.954, 2000.
751 Yu, H., Zhang, Q., Xu, C. Y., Du, J., Sun, P. and Hu, P.: Modified Palmer Drought
752 Severity Index: Model improvement and application, Environ. Int., 130(January),
753 104951, doi:10.1016/j.envint.2019.104951, 2019.

https://doi.org/10.5194/hess-2020-383
Preprint. Discussion started: 28 July 2020

754 Vogel, M. M., Zscheischler, J. and Seneviratne, S. I.: Varying soil moisture-atmosphere
755 feedbacks explain divergent temperature extremes and precipitation projections in
756 central Europe, Earth Syst. Dyn., doi:10.5194/esd-9-1107-2018, 2018.
757 Yuan, X., Wang, L., Wu, P., Ji, P., Sheffield, J. and Zhang, M.: Anthropogenic shift
758 towards higher risk of flash drought over China, Nat. Commun.,
759 doi:10.1038/s41467-019-12692-7, 2019.
760 Zhang, Q., Li, Q., Singh, V. P., Shi, P., Huang, Q. and Sun, P.: Nonparametric
761 Integrated Agrometeorological Drought Monitoring: Model Development and
762 Application, J. Geophys. Res. Atmos., 123(1), 73–88, doi:10.1002/2017JD027448,
763 2018.
764 Zhang, W. J., Lu, Q. F., Gao, Z. Q. and Peng, J.: Response of remotely sensed
765 normalized difference water deviation index to the 2006 drought of eastern
766 Sichuan Basin, Sci. China, Ser. D Earth Sci., 51(5), 748–758, doi:10.1007/s11430-
767 008-0037-0, 2008.
768 Zhang, Y., You, Q., Chen, C. and Li, X.: Flash droughts in a typical humid and
769 subtropical basin: A case study in the Gan River Basin, China, J. Hydrol., 551,
770 162–176, doi:10.1016/j.jhydrol.2017.05.044, 2017.
771 Zhang, Y., You, Q., Mao, G., Chen, C. and Ye, Z.: Short-term concurrent drought and
772 heatwave frequency with 1.5 and 2.0 °C global warming in humid subtropical
773 basins: a case study in the Gan River Basin, China, Clim. Dyn., 52(7–8), 4621–
774 4641, doi:10.1007/s00382-018-4398-6, 2019.
775 Zhong, R., Chen, X., Lai, C., Wang, Z., Lian, Y., Yu, H. and Wu, X.: Drought
776 monitoring utility of satellite-based precipitation products across mainland China,
777 J. Hydrol., 568(June 2018), 343–359, doi: 10.1016/j.jhydrol.2018.10.072, 2019a.
778 Zhong, R., Zhao, T., He, Y. and Chen, X.: Hydropower change of the water tower of

https://doi.org/10.5194/hess-2020-383
Preprint. Discussion started: 28 July 2020


Hydrology and Earth System Sciences
Discussions

779 Asia in 21st century: A case of the Lancang River hydropower base, upper
780 Mekong, Energy, 179, 685–696, doi:10.1016/j.energy.2019.05.059, 2019b.
781 Zscheischler, J., Michalak, A. M., Schwalm, C., Mahecha, M. D. and Zeng, N.: Impact
782 of large-scale climate extremes on biospheric carbon fluxes: An intercomparison
783 based on MsTMIP data, Global Biogeochem. Cycles, 28(6), 585–600,
784 doi:10.1002/2014GB004826, 2014.
785 Zscheischler, J., Orth, R. and Seneviratne, S. I.: Bivariate return periods of temperature
786 and precipitation explain a large fraction of European crop yields, Biogeosciences,
787 doi:10.5194/bg-14-3309-2017, 2017a.
788 Zscheischler, J. and Seneviratne, S. I.: Dependence of drivers affects risks associated
789 with compound events, Sci. Adv., 3(6), 1–11, doi:10.1126/sciadv.1700263, 2017b.
790 Zscheischler, J., Westra, S., Van Den Hurk, B. J. J. M., Seneviratne, S. I., Ward, P. J.,
791 Pitman, A., Aghakouchak, A., Bresch, D. N., Leonard, M., Wahl, T. and Zhang,
792 X.: Future climate risk from compound events, Nat. Clim. Chang., 8(6), 469–477,
793 doi:10.1038/s41558-018-0156-3, 2018.
794 Zscheischler, J., Martius, O., Westra, S., Bevacqua, E. and Raymond, C.: A typology
795 of compound weather and climate events, Nat. Rev. Earth Environ., doi:
796 https://doi.org/10.1038/s43017-020-0060-z, 2020.
797
798
799
800
801
802

https://doi.org/10.5194/hess-2020-383
Preprint. Discussion started: 28 July 2020

Hydrology and Earth System Sciences
Discussions

803 **Table**

804 Table 1 Categories of compound dry and hot conditions based on SCDHI.

Category	Dry and hot condition	SCDHI
G_0	Abnormal	(-0.80, -0.50]
G_1	Light	(-1.30, -0.80]
G_2	Moderate	(-1.60, -1.30]
G_3	Heavy	(-2.0, -1.60]
G_4	Extreme	≤ -2

805
806
807
808
809
810
811
812
813
814
815
816
817
818
819
820
821
822
823
824
825

https://doi.org/10.5194/hess-2020-383
Preprint. Discussion started: 28 July 2020

Hydrology and Earth System Sciences
Discussions
Open Access
EGU

826 **Figure**

827

828

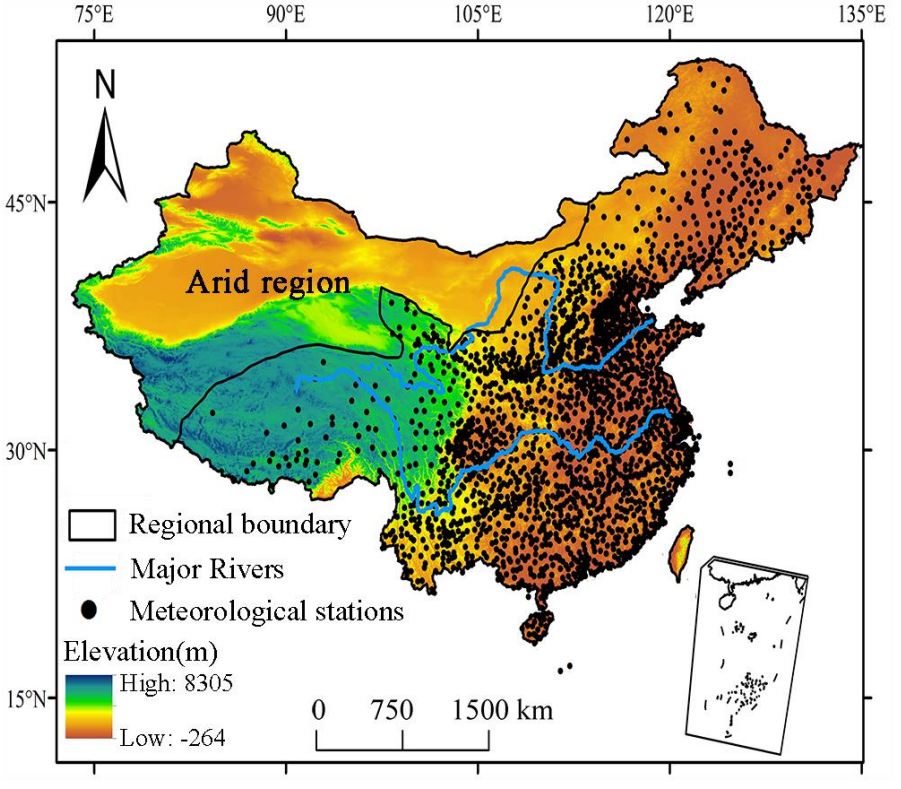

829

830 Figure 1 Geographical position of China and local of meteorological stations.

831

832

833

834

835

836

837

838

https://doi.org/10.5194/hess-2020-383
Preprint. Discussion started: 28 July 2020

Hydrology and Earth System Sciences
Discussions

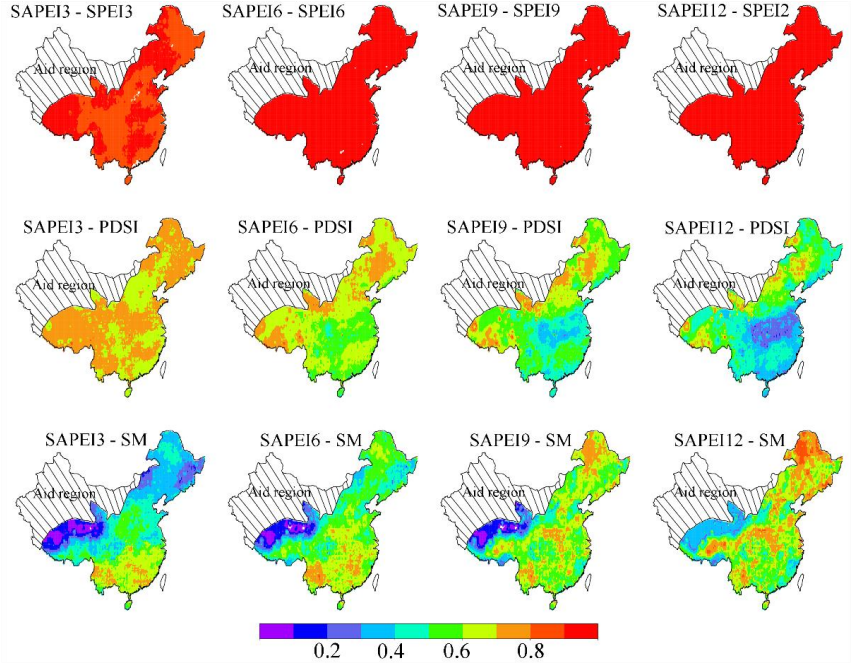

839

840 Figure 2 The spatial pattern of the correlations between monthly SAPEI and SPEI/PDSI,

841 and between daily SAPEI and soil moisture (SM). The monthly SAPEI is computed by

842 averaging the daily values in each month.

843

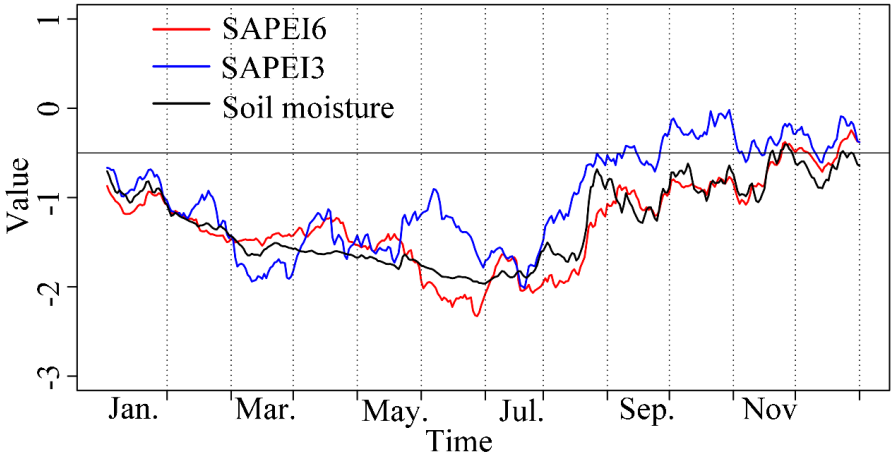

844

845 Figure 3 SAPEI (3- and 6-month) and soil moisture series during the 2009/2010 drought

846 event over the southwest China. The series were spatially average merged series.

https://doi.org/10.5194/hess-2020-383
Preprint. Discussion started: 28 July 2020

Hydrology and Earth System Sciences
Discussions

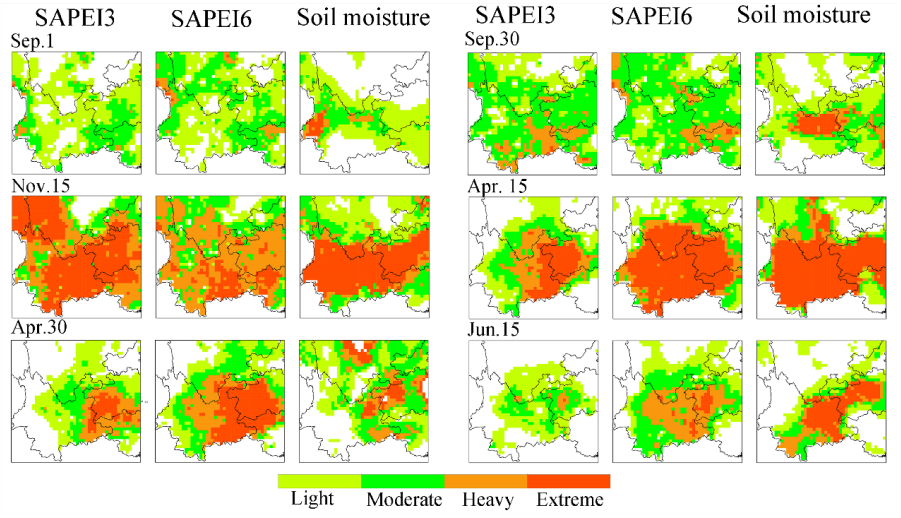

847

848 Figure 4 Daily evolutions of the 2009/2010 drought event over the southwest China

849 monitored by 3- and 6-month SAPEI and soil moisture.

850

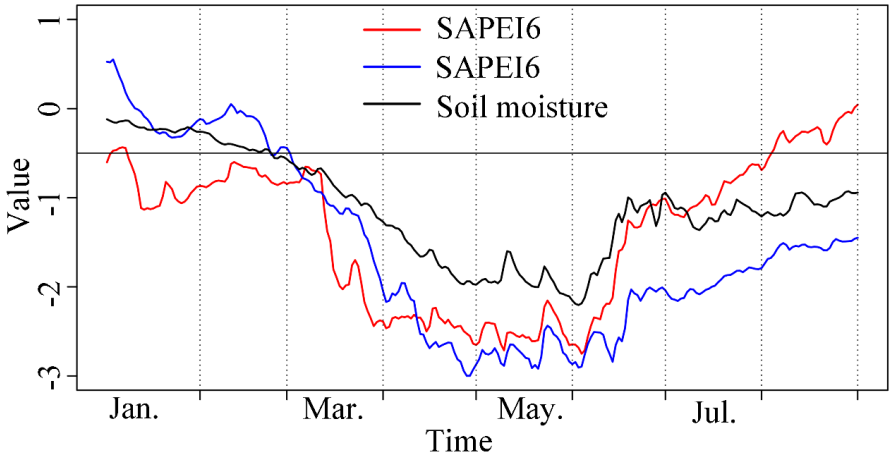

851

852 Figure 5 SAPEI (3- and 6-month) and soil moisture series during the 2011 drought

853 event over the middle and lower reaches of the Yangtze River. The series were spatially

854 average merged series.

855

856

857

https://doi.org/10.5194/hess-2020-383
Preprint. Discussion started: 28 July 2020

Hydrology and Earth System Sciences
Discussions

858
859
860

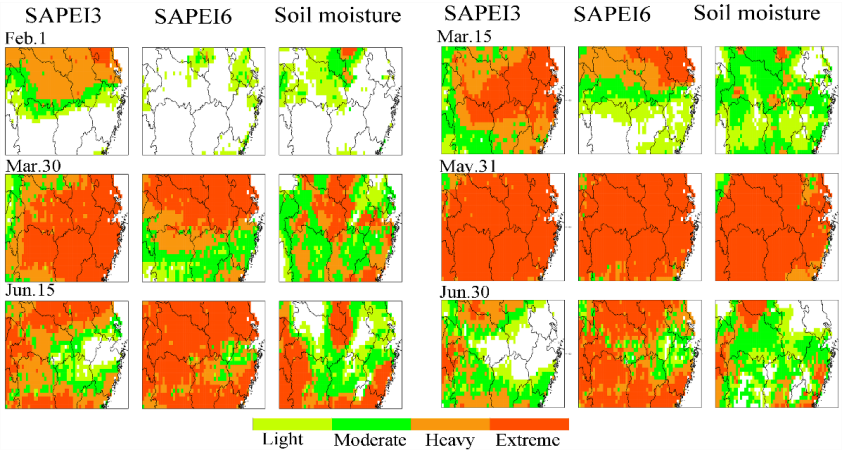

861

862 Figure 6 Daily evolutions of the 2011 drought event over the middle and lower reaches

863 of the Yangtze River monitored by 3- and 6-month SAPEI and soil moisture.

864
865

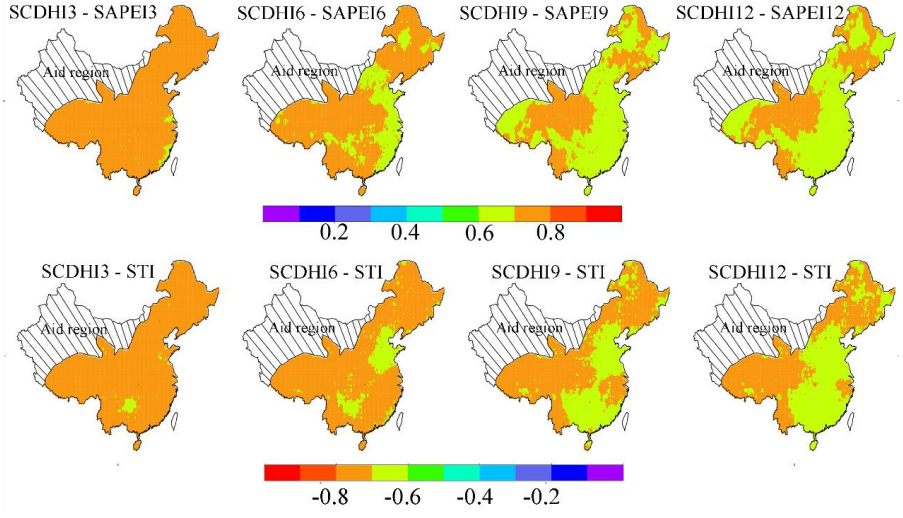

866

867 Figure 7 The spatial pattern of the correlations between SCDHI and SAPEI/STI at daily

868 scale from 1961 to 2018.

https://doi.org/10.5194/hess-2020-383
Preprint. Discussion started: 28 July 2020

Hydrology and Earth System Sciences
Discussions
Open Access
EGU

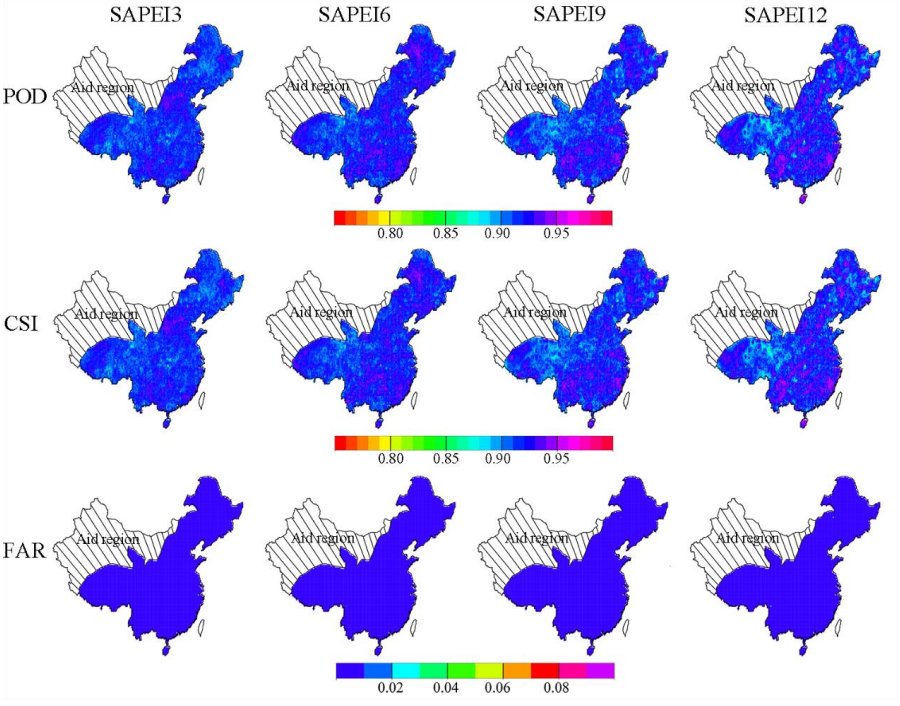

869

870 Figure 8 The spatial pattern of POD, FAR, and CSI for SCDHI at 3-, 6-, 9- and 12-

871 month time scales from 1961 to 2018.

872

https://doi.org/10.5194/hess-2020-383
Preprint. Discussion started: 28 July 2020

Hydrology and Earth System Sciences
Discussions
Open Access
EGU

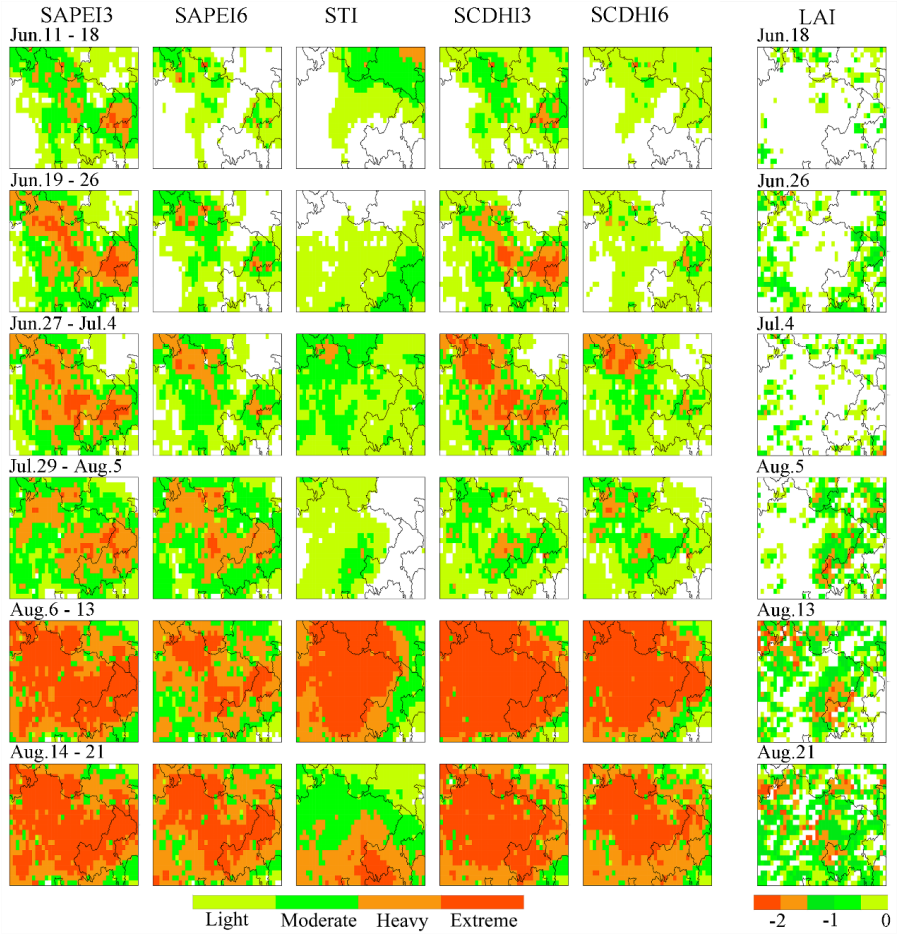

873

874 Figure 9. The spatial evolutions of the compound dry and hot event over the Sichuan-

875 Chongqing region in 2006 and its impact on vegetation.

876

877

878

879

880

881

https://doi.org/10.5194/hess-2020-383
Preprint. Discussion started: 28 July 2020

Hydrology and Earth System Sciences
Discussions
Open Access
EGU

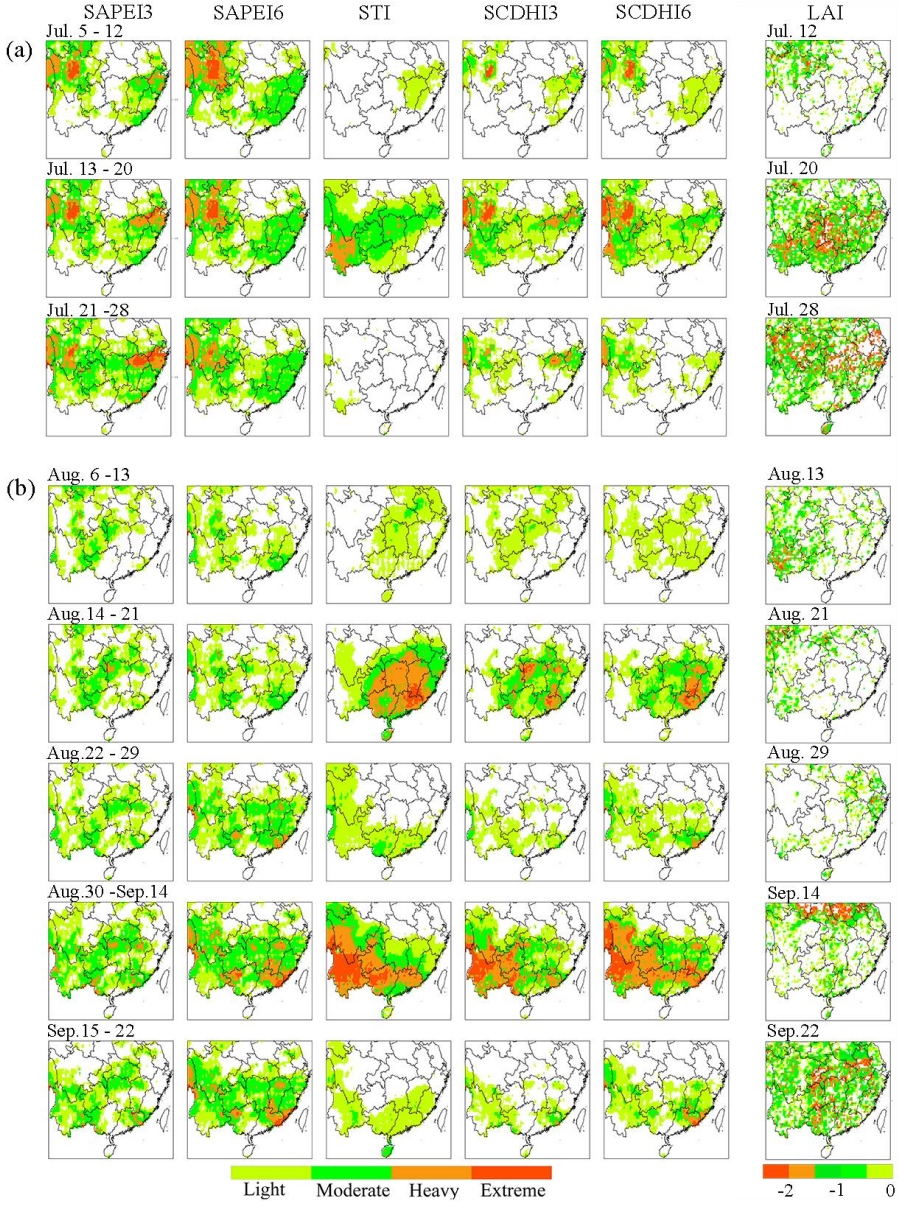

Figure 10 The spatial evolutions of the compound dry and hot event over the southern China in 2009 and its impact on vegetation.

https://doi.org/10.5194/hess-2020-383
Preprint. Discussion started: 28 July 2020

Hydrology and Earth System Sciences
Discussions
Open Access
EGU

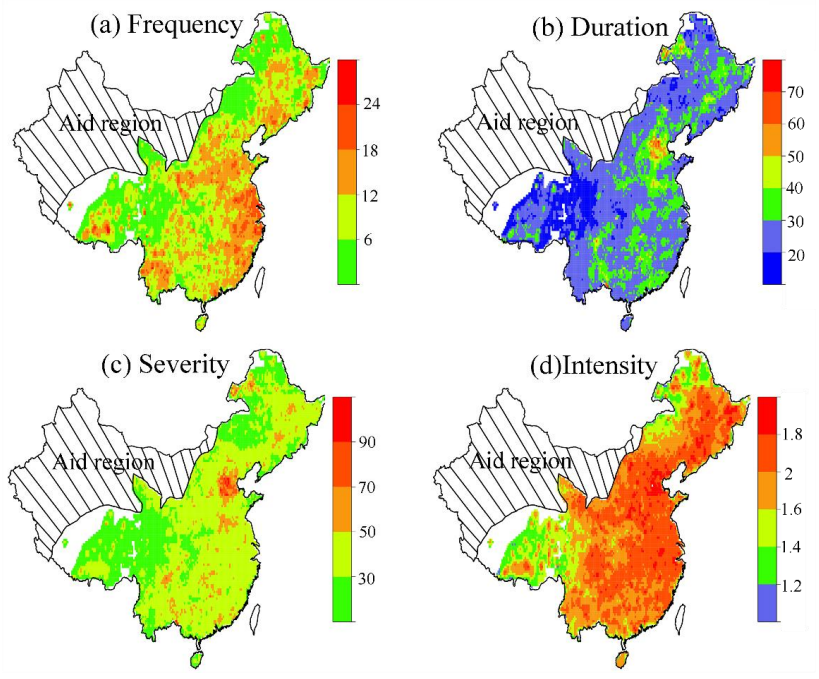

888

889 Figure 11 The spatial pattern of the characteristics of the compound dry and hot event

890 in China from 1961 to 2018.

891

892

893

894

895

896

897

898

https://doi.org/10.5194/hess-2020-383
Preprint. Discussion started: 28 July 2020

Hydrology and Earth System Sciences
Discussions

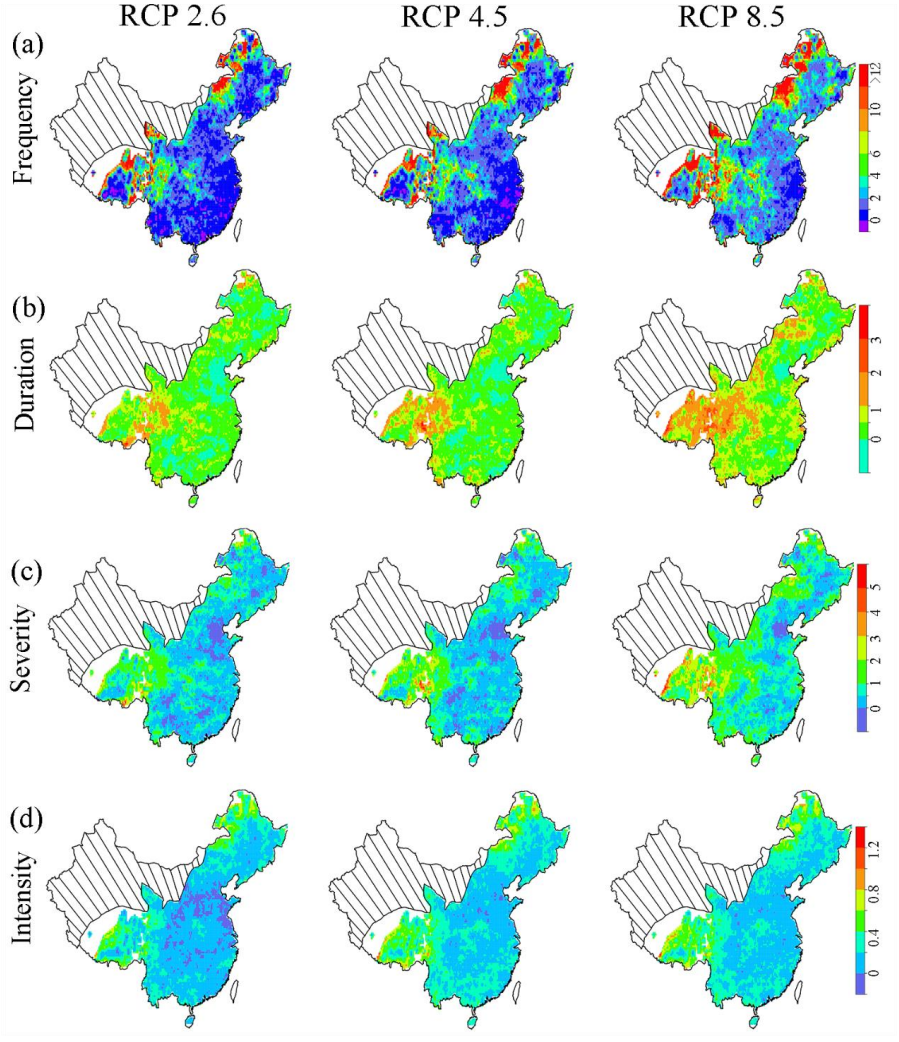

Figure 12 Future changes in characteristics of the compound dry and hot events under the RCP 2.6, RCP4.5 and RCP8.5 scenarios. The change values were the ratio of the future value to the reference values. Reference period: 1961-2018, and future period: 2050-2100.

https://doi.org/10.5194/hess-2020-383
Preprint. Discussion started: 28 July 2020

Hydrology and Earth System Sciences
Discussions
Open Access
EGU

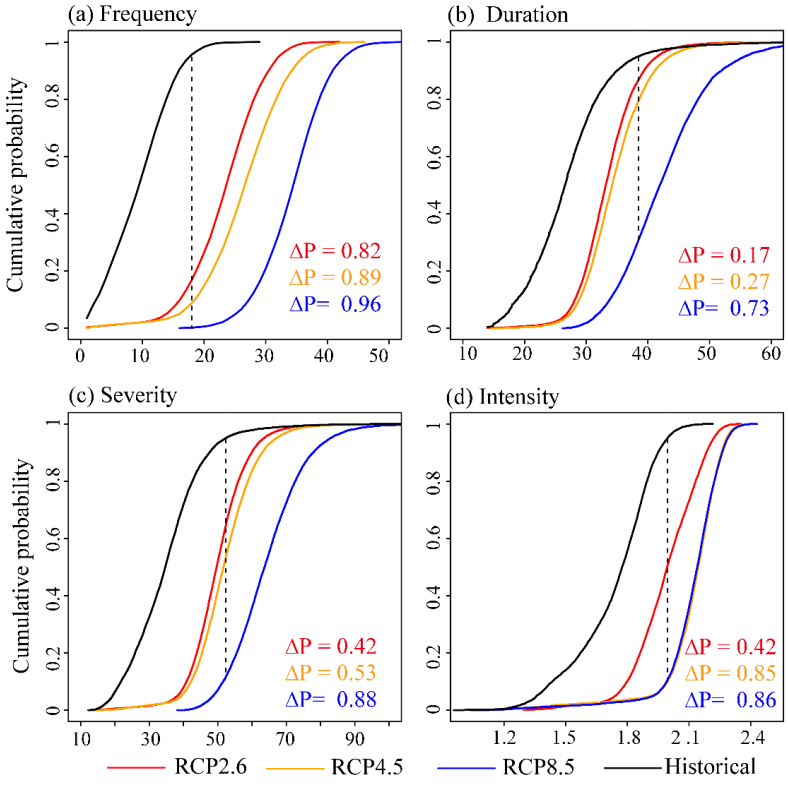

Figure 13 Cumulative probability functions of characteristics of the compound drought and hot events in historical and future period. The vertical lines denote the probability of the 95th percentile value during the historical period. ΔP denotes the changes in the probability of the 95th percentile value between the historical period and the future period. Reference period: 1961-2018, and future period: 2050-2100. The red, orange, and blue fonts refer to the change values under RCP 2.6, 4.5 and 8.5 scenario, respectively.